



# VU Research Portal

## Ultrafast double-pulse parametric amplification for precision Ramsey metrology

Kandula, D.Z.; Renault, A.A.L.; Gohle, C.; Wolf, A.L.; Witte, S.; Hogervorst, W.; Ubachs, W.M.G.; Eikema, K.S.E.

### ***published in***

Optics Express  
2008

### ***DOI (link to publisher)***

[10.1364/OE.16.007071](https://doi.org/10.1364/OE.16.007071)

### ***document version***

Publisher's PDF, also known as Version of record

### [Link to publication in VU Research Portal](#)

### ***citation for published version (APA)***

Kandula, D. Z., Renault, A. A. L., Gohle, C., Wolf, A. L., Witte, S., Hogervorst, W., Ubachs, W. M. G., & Eikema, K. S. E. (2008). Ultrafast double-pulse parametric amplification for precision Ramsey metrology. *Optics Express*, 16(10), 7071-7082. <https://doi.org/10.1364/OE.16.007071>

### **General rights**

Copyright and moral rights for the publications made accessible in the public portal are retained by the authors and/or other copyright owners and it is a condition of accessing publications that users recognise and abide by the legal requirements associated with these rights.

- Users may download and print one copy of any publication from the public portal for the purpose of private study or research.
- You may not further distribute the material or use it for any profit-making activity or commercial gain
- You may freely distribute the URL identifying the publication in the public portal ?

### **Take down policy**

If you believe that this document breaches copyright please contact us providing details, and we will remove access to the work immediately and investigate your claim.

### **E-mail address:**

[vuresearchportal.ub@vu.nl](mailto:vuresearchportal.ub@vu.nl)

# Ultrafast double-pulse parametric amplification for precision Ramsey metrology

D. Z. Kandula, A. Renault, Ch. Gohle, A. L. Wolf, S. Witte,  
W. Hogervorst, W. Ubachs, K. S. E. Eikema

*Atomic, Molecular, and Laser Physics Group, Laser Centre Vrije Universiteit, De Boelelaan  
1081, 1081 HV Amsterdam, The Netherlands*

[kjeld@nat.vu.nl](mailto:kjeld@nat.vu.nl)

**Abstract:** We demonstrate phase stable, mJ-level parametric amplification of pulse pairs originating from a Ti:Sapphire frequency comb laser. The amplifier-induced phase shift between the pulses has been determined interferometrically with an accuracy of  $\approx 10$  mrad. Typical phase shifts are on the order of 50-200 mrad, depending on the operating conditions. The measured phase-relation can be as stable as 20 mrad rms ( $1/300^{\text{th}}$  of an optical cycle). This makes the system suitable for Ramsey spectroscopy at short wavelengths by employing harmonic upconversion of the double-pulses in nonlinear media.

© 2008 Optical Society of America

**OCIS codes:** (190.4970) Parametric oscillators and amplifiers; (320.7090) Ultrafast lasers; (320.7160) Ultrafast technology; (350.5030) Phase

---

## References and links

1. M. Uiberacker, Th. Uphues, M. Schultze, A. J. Verhoef, V. Yakovlev, M. F. Kling, J. Rauschenberger, N. M. Kabachnik, H. Schröder, M. Lezius, K. L. Kompa, H.-G. Muller, M. J. J. Vrakking, S. Hendel, U. Kleineberg, U. Heinzmann, M. Drescher and F. Krausz "Attosecond real-time observations of electron tunnelling in atoms," *Nature (London)* **446**, 627–632 (2007)
2. M. F. Kling, Ch. Siedschlag, A. J. Verhoef, J. I. Khan, M. Schulze, Th. Uphues, Y. Ni, M. Uierbacker, M. Drescher, F. Krausz, and M. J. J. Vrakking "Control of Electron Localization in Molecular Dissociation," *Science* **312**, 246–248 (2006)
3. N. F. Ramsey "A Molecular Beam Resonance Method with Separated Oscillating Fields," *Phys. Rev.* **78**, 695–699 (1950)
4. S. Cavalieri, R. Eramo, M. Materazzi, Ch. Corsi, and M. Bellini, "Ramsey-Type Spectroscopy with High-Order Harmonics," *Phys. Rev. Lett.* **89**, 133002 (2002).
5. S. Witte, R. Th. Zinkstok, W. Ubachs, W. Hogervorst, and K. S. E. Eikema, "Deep-Ultraviolet Quantum Interference Metrology with Ultrashort Laser Pulses," *Science* **307**, 400–403 (2005).
6. R. Holzwarth, Th. Udem, and Th. W. Hänsch, "Optical Frequency Synthesizer for Precision Spectroscopy," *Phys. Rev. Lett.* **85**, 2264–2267 (2000).
7. D. J. Jones, S. A. Diddams, J. K. Ranka, A. Stentz, R. S. Windeler, J. L. Hall, and S. T. Cundiff, "Carrier-Envelope Phase Control of Femtosecond Mode-Locked Lasers and Direct Optical Frequency Synthesis," *Science* **288**, 635–639 (2000).
8. Ch. Gohle, Th. Udem, M. Herrmann, J. Rauschenberger, R. Holzwarth, H. A. Schuessler, F. Krausz, and Th. W. Hänsch, "A frequency comb in the extreme ultraviolet," *Nature (London)* **436**, 234–237 (2005).
9. R. J. Jones, K. D. Moll, J. Thorpe, J. Ye "Phase-Coherent Frequency Combs in the Vacuum Ultraviolet via High-Harmonic Generation inside a Femtosecond Enhancement Cavity," *Opt. Lett.* **29**, 2812–2814 (2004).
10. R. Th. Zinkstok, S. Witte, W. Ubachs, W. Hogervorst, and K. S. E. Eikema, "Frequency comb laser spectroscopy in the vacuum-ultraviolet region," *Phys. Rev. A* **73**, 061801 (2006).

11. A. J. Verhoef, J. Seres, K. Schmid, Y. Nomura, G. Tempea, L. Veisz, F. Krausz, "Compression of the pulses of a Ti:sapphire laser system to 5 femtoseconds at 0.2 terawatt level," *Appl. Phys. B* **82**, 513–517 (2006).
12. C. P. Hauri, W. Kornelis, F. W. Helbing, A. Heinrich, A. Couairon, A. Mysiorowicz, J. Biegert, U. Keller, "Generation of intense, carrier-envelope phase-locked few-cycle laser pulses through filamentation," *Appl. Phys. B* **79**, 673–677 (2004).
13. S. Witte, R. Th. Zinkstok, A. L. Wolf, W. Hogervorst, W. Ubachs, and K. S. E. Eikema, "A source of 2 terawatt, 2.7 cycle laser pulses based on noncollinear optical parametric chirped pulse amplification," *Opt. Express* **14**, 8168–8177 (2006).
14. A. Renault, D. Z. Kandula, S. Witte, A. L. Wolf, R. Th. Zinkstok, W. Hogervorst, and K. S. E. Eikema, "Phase stability of terawatt-class ultrabroadband parametric amplification," *Opt. Lett.* **32**, 2363–2365 (2007).
15. M. B. Gaarde, F. Salin, E. Constant, Ph. Balcou, K. J. Schafer, K. C. Kulander, and A. L'Huillier, "Spatiotemporal separation of high harmonic radiation into two quantum path components," *Phys. Rev. A* **59**, 1367–1373 (1999).
16. I. N. Ross, P. Matousek, G. H. C. New, and K. Osvay, "Analysis and optimization of optical parametric chirped pulse amplification," *J. Opt. Soc. Am. B* **19**, 2945–2956 (2002).
17. S. Witte, R. Th. Zinkstok, W. Hogervorst, and K. S. E. Eikema, "Numerical simulations for performance optimization of a few-cycle terawatt NOPCPA system," *Appl. Phys. B* **87**, 677–684 (2007).
18. M. Takeda, H. Ina, and S. Kobayashi, "Fourier-transform method of fringe-pattern analysis for computer-based topography and interferometry," *J. Opt. Soc. Am.* **72**, 156–160 (1982).
19. Pearson's linear correlation coefficient is not appropriate, as it assumes a linear relationship between the variables, which is not the case here.
20. The phase mismatch is very sensitive to the angles in the parametric amplification. It is extremely difficult to measure them accurate enough to be able to determine  $\Delta k$ .

## 1. Introduction

High-power phase-controlled ultrashort laser pulses are essential for various applications, such as attosecond science [1], quantum control of molecular dynamics [2] and Ramsey spectroscopy [3, 4, 5]. Stabilization and control of the phase  $\phi_{CE}$  between the field and envelope of low power oscillator pulses was demonstrated several years ago [6, 7] and has revolutionized the measurement of optical frequencies. The frequency comb technique has become a standard tool for spectroscopy in many laboratories across the world. The spectral range of frequency comb lasers is typically in the near-infrared, but can be extended through nonlinear interactions. One example is the generation of harmonics from frequency comb laser pulses to extend the spectrum to the extreme ultraviolet (XUV). Aiming at Ramsey spectroscopy of Helium at  $\approx 50$  nm, we pursued the amplification of two subsequent pulses from such a laser to an energy level suitable for generation of the desired wavelength. Direct excitation with the upconverted pulses should allow measurement of the ground state energy of helium and hydrogen-like atoms with an unprecedented precision for tests of e.g. quantum-electrodynamics. The minimum requirements for such an experiment are two phase-coherent pulses with enough intensity to generate harmonics. One approach is to use a Michelson interferometer to split an amplified pulse in two, as is e.g. done in [4]. The drawback of this method is that the resolution is limited by the calibration of the pulse delay and by the stability of the interferometer. An interesting technique that avoids those problems was demonstrated in [8, 9], where an external cavity was used to build up the desired power level for high-harmonic generation from a frequency-comb pulse train. Alternatively, one can amplify multiple subsequent pulses from a frequency comb laser for harmonic upconversion. With pulses amplified to a level of tens of  $\mu\text{J}$ , high-resolution direct frequency comb spectroscopy was demonstrated at 212 nm and 125 nm [5, 10]. To reach the XUV spectral region a higher pulse energy is required.

Phase-stable amplification of single ultrashort pulses using Ti:sapphire amplifiers [11, 12] and parametric amplification [13, 14] has been demonstrated before. For Ramsey-type experiments the latter approach is advantageous, as it is theoretically capable of amplifying two subsequent pulses in the same way while maintaining saturation for each pulse. It also gives more freedom in choosing the output spectrum. Here we show that noncollinear optical chirped pulse amplification (NOPCPA) can indeed be extended to two-pulse amplification (with a time

separation of 6.6 ns) while maintaining a high mutual phase stability. This phase stability is one of the key issues, and therefore investigated in detail, as any phase deviation will be multiplied in harmonic upconversion to the extreme ultraviolet. Also the stability of the amplified pulses has been investigated because variations in the intensity can induce additional phase shifts in the harmonic generation process itself [15].

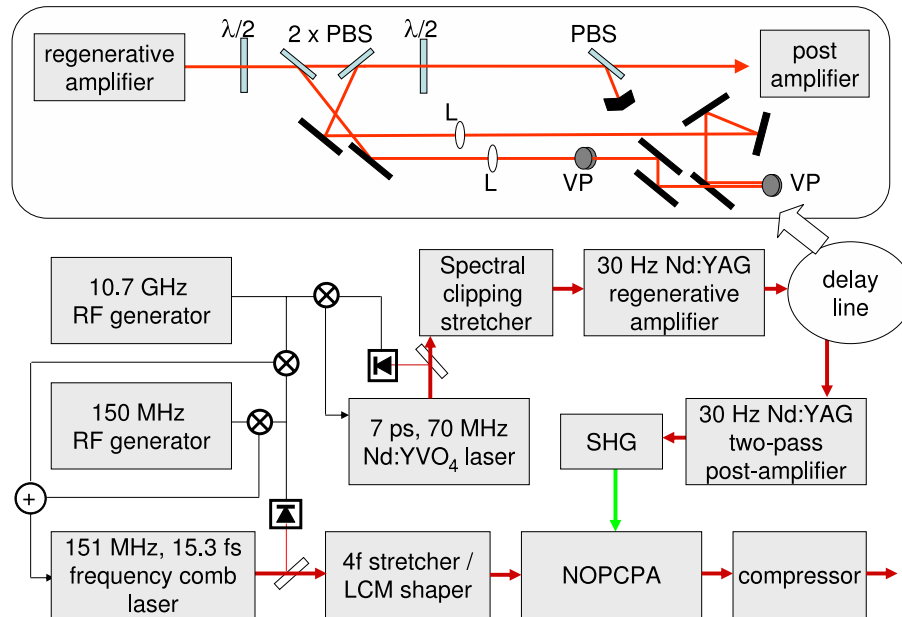


Fig. 1. Schematic of the noncollinear optical parametric chirped pulse amplifier (NOPCPA), showing in detail the relay imaged delay line that splits the pulses in two replica. PBS: polarizing beam splitter, VP: vertical periscope, LCM: liquid crystal modulator, L: relay image lens  $f = 50\text{cm}$ , SHG: second harmonic generation

In contrast to the previous working conditions of our NOPCPA system (where we generated single laser-pulses with a spectral width of  $\approx 300\text{ nm}$  [13]) we limited the spectral width of the pulses to  $30\text{ nm}$ . This bandwidth is a good compromise between harmonic conversion efficiency and spectral power density in the XUV, and it reduces complications due to wavelength dependence of the phase [14]. This is the condition that will be used for harmonic generation in later experiments. As a result the energy per pulse is  $1 - 2\text{ mJ}$ . The phase shift relative to the comb laser of the two pulses induced by the amplification has been measured using spectral interferometry in a Mach-Zehnder interferometer. In addition the spatial dependence has been investigated, as well as the influence of unequal amplification of the two pulses on their relative phase.

## 2. Amplification of pulse pairs

Ramsey spectroscopy requires a well known and stable phase relationship between the pulses used for excitation of a transition. We make sure that this is the case by employing the pulses from a frequency comb laser as a seed for the NOPCPA. However, optical parametric amplification can induce a phase shift depending on the phase-matching conditions of the amplifier and the intensity of the pump pulse [14, 16, 17]. The phase of the amplified seed pulse  $\varphi_s$  is given by [16]:

$$\varphi_s(L) = \varphi_s(0) - \frac{\Delta k}{2} \int_0^L \frac{f}{f + \gamma_s^2} dz \quad (1)$$

Here the fractional pump intensity depletion is defined as:  $f = 1 - I_p(z)/I_p(0)$  and  $\gamma_s^2 = \omega_p I_s(0)/\omega_s I_p(0)$ .  $I_p$  and  $I_s$  are the intensity of the pump and the seed respectively, while  $\omega_p$  and  $\omega_s$  are the corresponding angular frequencies.  $L$  is the length of the parametric interaction. A change in the alignment in the range of  $0.01^\circ$  for the noncollinear angle between pump and seed changes the phase of the amplified pulse on the order of 0.3 rad after 5 mm of propagation in the BBO-crystal. Amplification in a NOPCPA of two subsequent laser pulses from the oscillator requires two strong pump pulses separated by the period of the frequency comb. Because of the reasons stated above, these two pulses need essentially the same intensity profile and wave front. We realized this by a modification in the pump laser of the previously demonstrated single pulse NOPCPA system [13].

The starting point of the pump laser is a Nd:YVO<sub>4</sub> oscillator, emitting 7 ps pulses at a repetition rate of 70 MHz. Clipping the spectrum stretches the pulses to  $\approx 100$  ps duration. The stretched pulses are amplified at 30 Hz repetition rate in a diode-pumped regenerative Nd:YAG amplifier, where the energy is boosted to 2 mJ per pulse. The required two pump pulses are produced by implementing a delay line behind the regenerative amplifier, where part of the energy is split off, delayed and recombined with the original beam using polarizing beam splitters. The total arm length of the delay line is  $\approx 2$  m, and corresponds exactly to the pulse delay of the comb laser of 6.6 ns. Figure 1 shows a scheme of the laser system together with a detailed layout of the delay line.

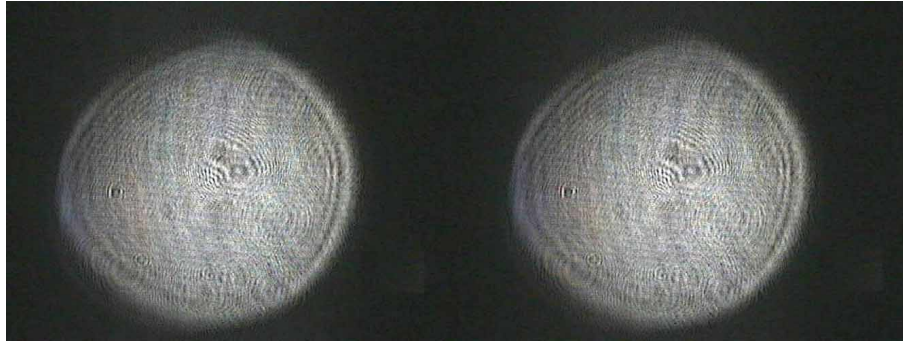


Fig. 2. Spatial profiles of the 1st and 2nd pump pulse after the post-amplifier. The small diffraction patterns are due to dust particles on the camera and other optics, and are not part of the actual beam profile.

Since the NOPCPA is very sensitive to the alignment (see e.g. [17]) the two pulses generated by the delay line need to have identical wave fronts and spatial profiles. This is achieved by a 4f relay-imaging system in the delay arm. The image inversion of the 4f system is counteracted by using an odd number of mirror reflections together with two vertical periscopes. To meet the requirements for precise identical alignment of the two pump pulses in NOPCPA, they are compared on a CCD camera behind the postamplifier at a distance of 6 m after the delay line in the relay-image plane, and at 9 m distance out of the relay-image plane. Figure 2 gives an example of the spatial profiles of the two pump pulses 9 m after the delay line, showing that they are essentially indistinguishable after this procedure. In this Mach-Zehnder arrangement half of the power is lost when projecting the pulses onto a common polarization, so that each of them contains 0.5 mJ of energy. The resulting beam is enlarged and sent into a flash-lamp

pumped Nd:YAG postamplifier (Fig. 1), where it reaches 180 mJ per pulse at 1064 nm. The relative intensity between the pulses can be adjusted using the half-wave plate in front of the delay line to compensate for the gain depletion seen by the second pulse in the postamplifier. Seeding the postamplifier with 50% more energy in the second pulse leads to equal output energy for both pulses.

Making the power and direction of the pump pulses the same is not yet enough for proper amplification. The time between the pulses must match the round-trip time in the frequency-comb oscillator exactly. This means that the repetition rate of the frequency-comb oscillator must be adjusted as the relay-image condition fixes the delay-line length. After coarsely setting it to the right value, we scan the delay between the seed and the pump beam in the NOPCPA while looking at the power level of the amplified pulses. If the delay between the seed pulses does not match the delay between the pump pulses, the ratio between them will vary after amplification. This information is used for fine-tuning the repetition rate of the frequency comb, until both pulses are amplified in the same way. The result is a stable intensity ratio between the amplified pulses on a level of 3% – 6% rms. Figure 3 shows typical energy traces of the two amplified pulses together with their ratio.

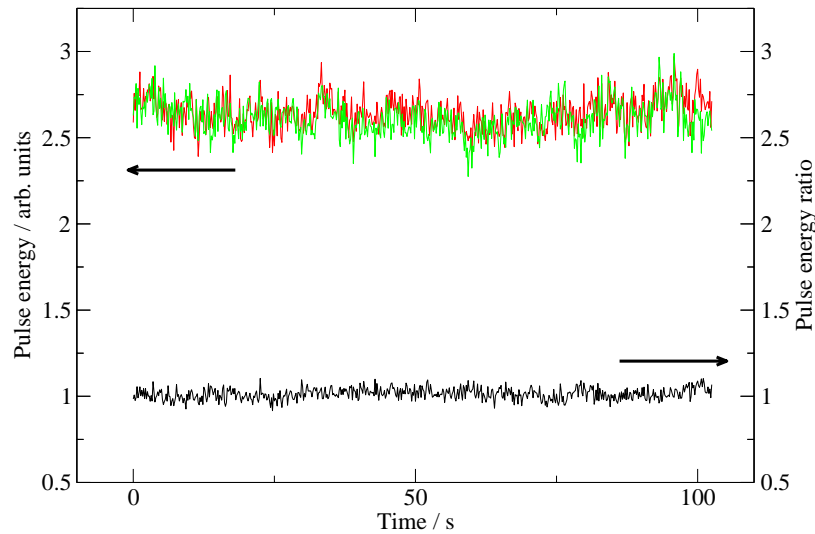


Fig. 3. Energy of the first and second amplified pulse (upper, red and green traces) and the ratio between them (lower, black trace). The energy stability here is 3.6% and 3.8% rms for the first and second pulse respectively and 3.3% rms for the ratio between them.

### 3. Measurements of the amplifier phase shift

The phases after amplification are measured relative to the frequency comb pulses with a Mach-Zehnder interferometer, as depicted in Fig. 4. In this setup half of the seed beam is sent into the NOPCPA, while the other half is split off as a reference. This reference is combined with a small fraction of the amplified pulses on a 5% beam splitter and sent through a single-mode optical fiber. Thus the mode profiles of the two beams are filtered and a perfect overlap of the amplified and reference pulses after the interferometer is established.



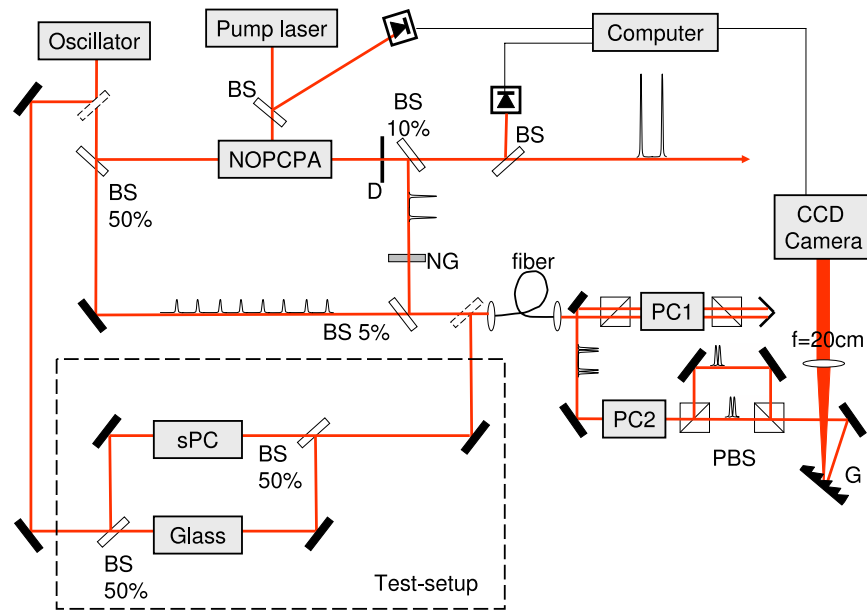


Fig. 4. Mach-Zehnder interferometer for measurement of the differential phase shift accumulated during the amplification in a NOPCPA, and the setup used to test the reliability of the measurement (dashed box). BS: Beam splitter, PBS: polarizing beam splitter, PC1/2: Pockels cells, sPC - slow Pockels cell, NG: neutral grey filter, D: diaphragm, G: 1200 l/mm grating

The amplified pulses are delayed with respect to the reference by about 1 ps, causing spectral interference in the combined beam. The interference fringes are detected with a spectrometer consisting of a CCD camera, a lens ( $f=20$  cm) and a grating with 1200 l/mm. A Pockels cell (PC1) is used to select only the two pulses from the oscillator that give an interference signal. This Pockels cell is double-passed to provide a contrast better than 10000 : 1 within a bandwidth of 30 nm, rendering the background due to other oscillator pulses essentially invisible within the exposure time of the camera ( $3\mu s$ ).

The two signal-reference pulse pairs are separated spatially using a second Pockels cell (PC2) and polarizing beam splitters in order to be able to analyze the interference patterns individually (see Fig. 5). The phase of the recorded fringes is determined using a Fourier transform based method, as described in [18]. This method determines the phase as a function of wavelength for every interferogram. By integrating this phase over a certain range and dividing it by the number of data points used, a single value for the phase is obtained, which reflects the actual position of the interference pattern. This phase of the fringes depends on many possible effects, which need to be taken into account in order to extract the influence of the amplification. These are: the alignment of the interferometer and fluctuations thereof, the actual part of the wavefront coupled into the fiber, nonlinear phase shifts in the fiber, spatial and temporal inhomogeneity of the Pockels effect, the contrast of the separation in PC2, and finally the phase shift induced in the NOPCPA. In the following we give a detailed overview of how these issues are dealt with.

The phase shift of the interferograms is determined mainly by the relative lengths of the  $\approx 10$  m long interferometer arms, which can vary by a few  $\mu m$  due to environmental influence. However, these variations are virtually identical for both pulse pairs, due to the small temporal delay (6.6 ns) between them. Therefore they cancel when evaluating the phase difference between the upper and the lower interferogram.

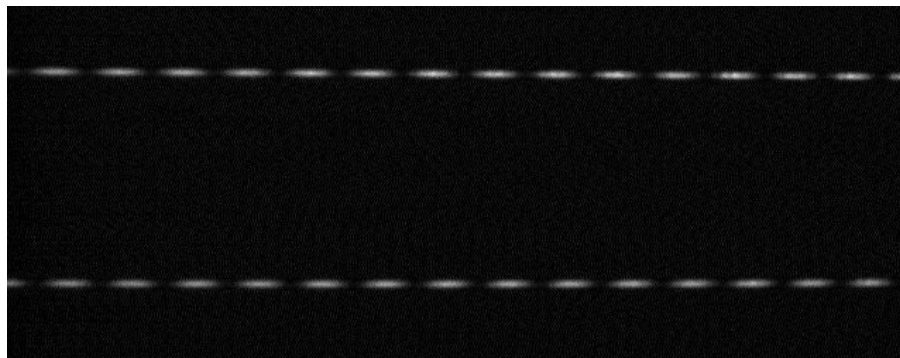


Fig. 5. Spectral interference fringes between the two amplified pulses and their respective reference pulses

Misalignment of the two beam paths after PC2 can lead to a small horizontal shift of the two fringe patterns. To cancel this effect and extract only the relative phase shift of the amplified pulses we employ an alternating switching scheme: In one configuration the polarization of the first pulse is rotated, the other configuration rotates the polarization of the second pulse. In this way we can exchange the paths of the first and second pulse towards the CCD, which means that we exchange the contribution of the NOPCPA phase shift on the phase of the fringes, but not the contribution of the alignment. This switching is performed every five seconds. The differential phase shift of the amplification can be now determined by subtracting the detected phase differences for both cases from each other. The contribution of the alignment disappears in the obtained phase trace, while the differential phase shift changes for the two switching positions of PC2. The resulting phase traces show a characteristic shape of a rectangular function, where a difference between the upper and the lower value gives *two* times the differential phase shift between the first and second pulse amplified in the NOPCPA (see e.g. the lowest, black trace in Fig. 6.)

As mentioned before, when using the source for high harmonic generation, any phase shift is multiplied by the harmonic order factor. Therefore a high accuracy better than  $1/200^{th}$  of an optical cycle in the infrared is required to identify the upconverted frequency comb mode in the XUV that is involved in the Ramsey excitation. The desired accuracy asks for additional testing of our measurement technique. We have performed such tests, using a Mach-Zehnder interferometer with a slow Pockels cell (sPC) instead of the NOPCPA in one of its arms (dashed box in Fig. 4). The Pockels cell was turned by  $45^\circ$ , to make it work as an electro-optic phase modulator without changing the polarization of the passing beam. It has a relatively long switching time of 60 ns in comparison to the time between the pulses. This still can produce small differential phase shifts in subsequent laser pulses traveling through the sPC. Two pulses are selected as in the normal measurement with PC1 and the introduced phase shifts are measured in two different ways. In one case the sPC in the interferometer is switched on and off, alternating between each measurement. The spectral interference between the pulse and its replica is recorded in a single interferogram that moves back and forth, corresponding to the phase shift induced by the sPC (see Fig. 6, the red and green traces). The differential phase shift between two subsequent pulses can be determined from two such measurements (one for each pulse). The comparison to the value measured instantaneously with the PC2-switching method used to determine phase shifts induced by the NOPCPA, gives a difference in the order of 5 mrad, confirming the reliability of the measurement method. Furthermore, comparing the spread in the values measured with the test scheme and the PC2-switching scheme (80 mrad rms and 10 mrad rms respectively, see



Fig. 6, measurement time: 90 s), demonstrates the high precision of the method used. Another test was performed measuring a zero phase shift by keeping the sPC in the interferometer off. The result was a phase shift of  $(-0.001 \pm 0.002)$  rad.

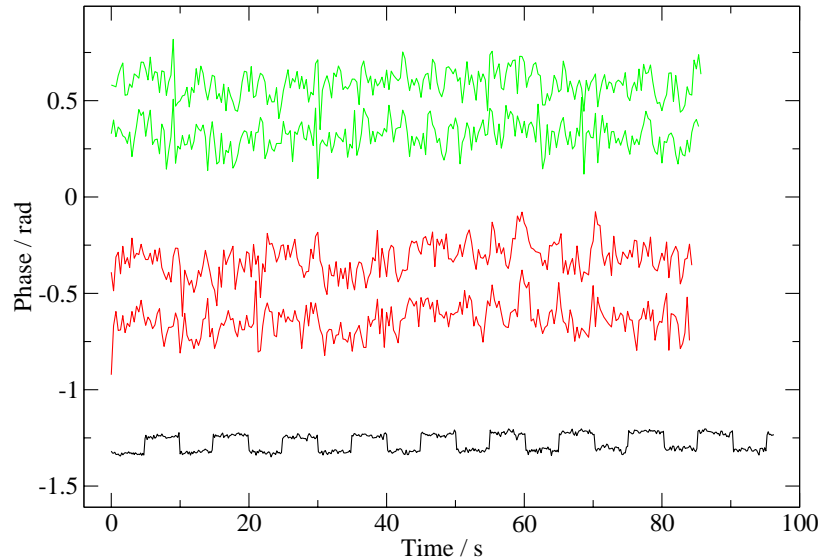


Fig. 6. Artificial phase shift measured with the interferometric switching technique (black/lower trace) and tested in a single interferogram for each pulse, with alternate switching the phase shift on and off (first pulse - green/upper traces, second pulse - red/middle traces).

PC2, which is used to separate the pulses before projecting them on the CCD camera, has a switching time of  $\approx 5$  ns, which is very close to the temporal separation of the pulses (6.6 ns). This leaves a possibility for the pulses to leak fractionally into the other channel, due to the imprecise time delays introduced by the Pockels cell electronics. We have investigated the possible influence of such behavior by setting the switching point of the Pockels cell PC2 to slightly wrong positions on purpose. Using pulses with a differential phase shift of 55 mrad we could only see a significant effect if the amount of light leaking into the wrong channel became comparable to the pulse itself (20% or more). Under normal operating conditions (5% leakage) the effect can be neglected.

Another possible source of error can be the optical fiber, used for cleaning the mode profile and perfect overlap of the amplified and reference pulses in the Pockels cells. Sending ultra-short pulses through an optical fiber with a core diameter of  $3\mu\text{m}$  may change the phase of the investigated pulses due to self phase modulation. The phase of each pulse could change in a different way, if they differ in intensity. To investigate this, we moved the slow Pockels cell (sPC) from the test setup (Fig. 4) into the beam before the interferometer. Despite the slow switching time of this device we could change the intensity of subsequent pulses using a polarizer to a ratio of 5 : 4. Doing this in front of the interferometer makes sure that the phase shift in the interferometer is zero, if nonlinear effects in the fiber have no influence. The differential phase shift was measured with an intensity ratio between the two interferometer arms of 1 : 2 and no phase deviations have been detected.

The result of these tests is that the single-shot accuracy of the interferometer technique is

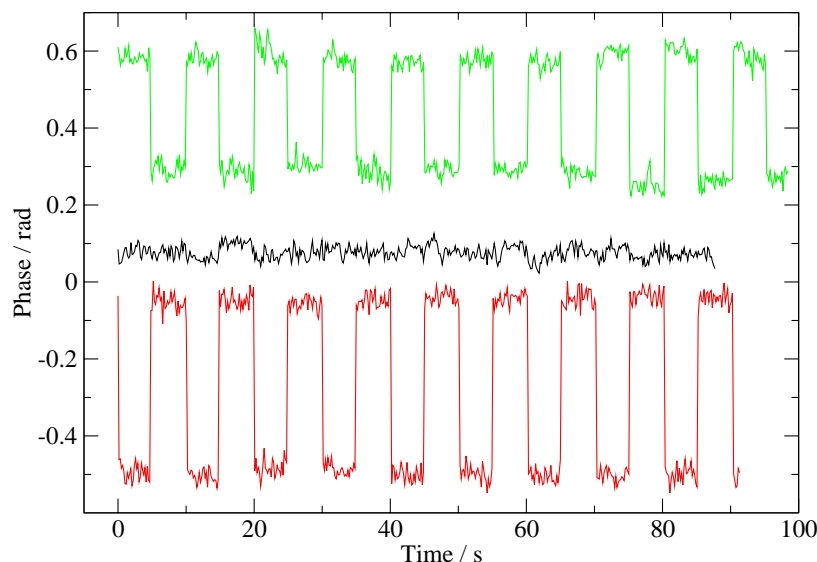


Fig. 7. Phase traces, measured on three different days, showing two times the difference in phase shift of 151 mrad (upper/green trace),  $-227$  mrad (lower/red) and  $-4$  mrad (black/middle trace).

better than 10 mrad. With this knowledge we investigated the influence of the NOPCPA on the phase of the pulses under different circumstances; in particular the stability of the phase between the pulses, spatial homogeneity, spectral dependence and the influence of unequal amplification on the phase shift.

Figure 7 shows three typical examples of a phase shift difference measured under normal operating conditions. These examples are taken from measurement series recorded on three different days, corresponding to slightly different alignments of the NOPCPA. The upper (green) trace corresponds to a difference in phase shift of 151 mrad with a rms variation over the measurement interval of 22 mrad. The difference in the lower (red) trace is as big as  $-227$  mrad with a variation of 20 mrad rms. The black trace in the middle shows a phase shift of  $-4$  mrad between the pulses and a variation of 16 mrad rms. Despite the relatively big change in the phase-shift difference of  $\approx 380$  mrad, the measured values spread only by 70 mrad (peak-peak) during the day. Notice that the short term stability of the differential phase shift does not depend on its actual value.

A dependence of the differential phase shift on the intensities of the pump pulses is expected from Eq. (1) and as well from the single pulse phase measurements performed previously [14]. We have investigated this for several operating conditions of the parametric amplifier. The influence of different intensities of the pump pulses on the phase shift is illustrated in Fig. 8. We have measured in three situations: one with equal pump power for both pulses and two with a ratio between the pump-pulses set such, that one seed pulse is amplified to half the energy of the other one. It results in three different values for the phase shift:  $-114$  mrad for two equal pulses,  $-270$  mrad and  $32$  mrad, for the first pulse stronger and second pulse stronger respectively. This behavior qualitatively confirms the model of NOPCPA presented in [16]. For normal (stable) operating conditions of the NOPCPA (see Fig. 3) the phase-intensity coupling is too small to be observed. In contrast, Fig. 9 shows a case with an unstable phase shift (red/lower trace) emerging from an exceptionally unstable ratio between the amplified pulses

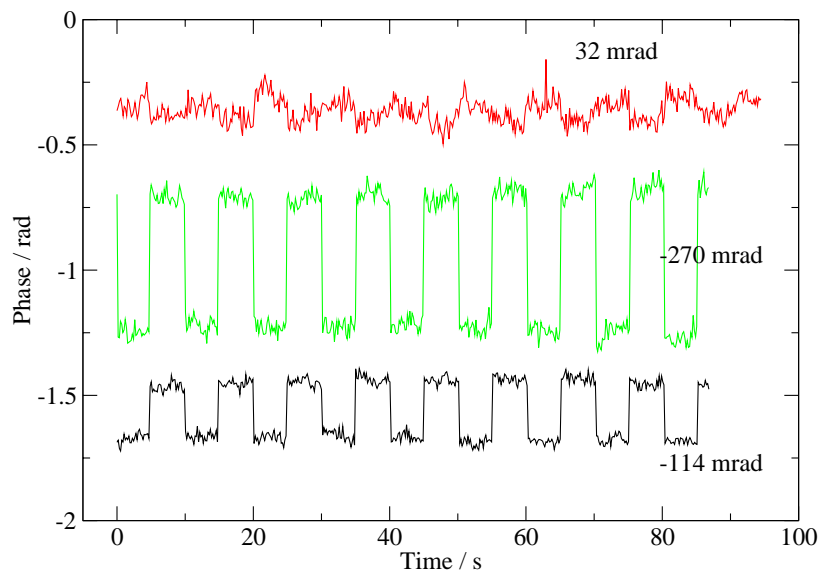


Fig. 8. Different phase shifts of  $-114$  mrad,  $32$  mrad and  $-270$  mrad, emerging from different pump-intensity ratios between two pulses (equal pulses (black), second pulse stronger (red) and first pulse stronger (green) respectively with a ratio of 2:1).

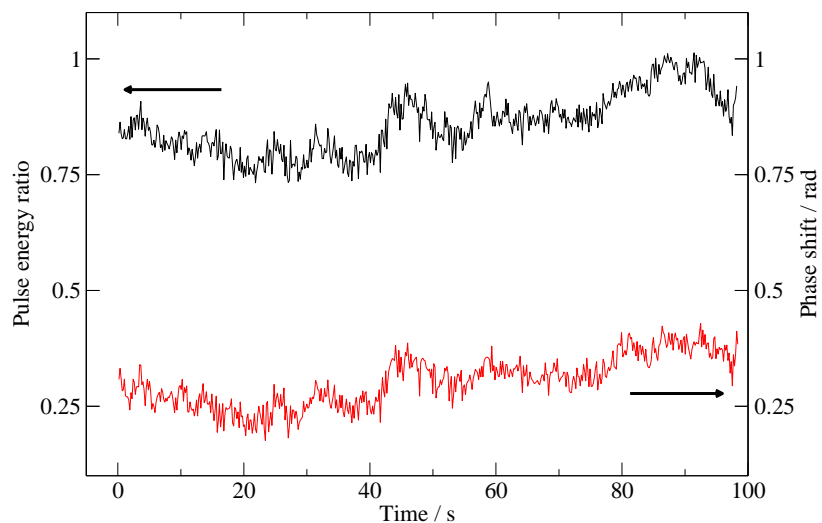


Fig. 9. Ratio between the energies of the first and second amplified pulse (black/upper trace) and the measured phase shift (red/lower trace)

(black/upper trace). The Spearman rank-order correlation coefficient [19] gives in this case a clear correlation of  $r = 0.95$ .

The phase mismatch  $\Delta k$  is a function of the seed wavelength [17], which can lead to differ-

ent phase shifts during amplification for different spectral components (see Eq.(1)). We have investigated this dependence for changes of the phase of single pulses in our previous measurements [14] with a broad spectrum. In the present situation the spectrum of the amplified pulses is relatively narrow (30 nm) and most of it (20 nm) covers the CCD-Camera in the interferometer. This allows us to compare the differential phase-shifts of different spectral components, selecting the corresponding parts of the recorded interferograms for the analysis. The analysis of the differential phase shifts in three spectral regions with a width of 3 nm around 790 nm, 793 nm and 796 nm respectively, shows small deviations (typically  $< 10$  mrad) from the mean values obtained by analyzing the whole spectral range at once. The deviation from the mean value is least for the central wavelength of the pulses and goes in opposite directions for the outer regions.

From Eq. (1) it can be seen that the induced phase shift depends on the phase mismatch  $\Delta k$  (which is inaccurately known [20]) and the fractional depletion of the pump beam. The latter depends strongly on the intensity of the pump beam, which also determines the conversion efficiency in the parametric process. A higher starting intensity will usually deplete the pump beam quicker, causing a bigger phase shift in the amplified pulses. Because the pump-pulse depletion in the first pass is negligible, hardly any phase shift is expected to occur there. In the second pass, however, there is more pump depletion and the pump beam is simply imaged (instead of relay imaged) onto the crystal, resulting in a significant divergence of the beam in the crystal. This leads to different noncollinear angles across the beam and therefore suboptimal conditions for parametric amplification. The contribution from this stage to the differential phase shifts was checked, by comparing it with and without the last stage of the amplifier. The amplification in the last crystal can be easily switched off by rotating the polarization of the pump beam therein. The measurements indeed confirm the expectations, giving a differential phase shift of  $-109$  mrad for the whole NOPCPA and  $-125$  mrad for the first two passes only. With a different alignment of the amplifier we detected a phase shift of  $-77$  mrad in three passes and the same value without amplification in the last crystal. This is strong evidence for the assumption that the second amplification stage is the major source of the observed differential phase shifts.

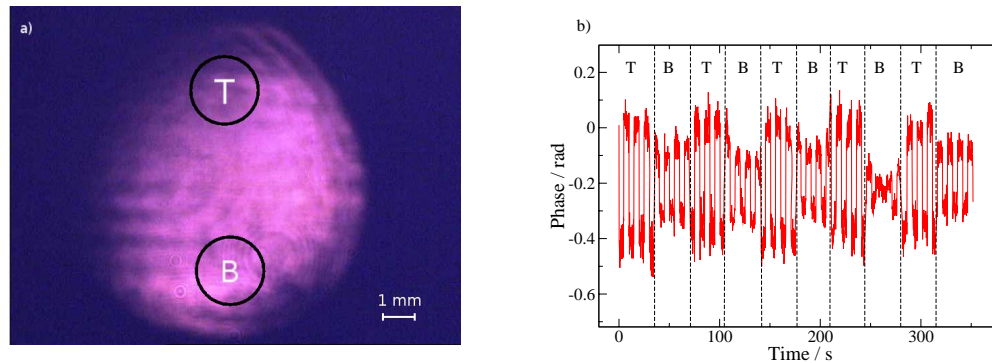


Fig. 10. a) Intensity profile of the amplified pulses after the last amplification stage. The circles refer to the beam sections chosen for the measurement, depicted in: b) Measurement of the phase-shift difference for two sections of the amplified pulse pair (as indicated in 10 a). The dashed lines indicate the switching between the two sections. T/B - top/bottom section.

Finally, in a series of measurements we have investigated differential phase shifts in different sections of the amplified beam. Those phase shifts can vary up to  $\approx 100$  mrad across the beam or be as low as  $\approx 30$  mrad, depending on the alignment of the amplifier. The measured

variation across the beam is of the same order of magnitude as the variations during a day at a fixed position in the beam profile. To detect whether the changes in phase really correspond to the chosen beam section (and not the time when they are measured), we took a series of measurements while switching between two positions in the beam during the data acquisition. Figure 10 b shows a phase trace taken by alternating the measured section between the two positions marked in Fig. 10 a. The phase shift in this case is  $-192$  mrad in the upper part of the beam and  $-95$  mrad in the lower section. This measurement clearly shows the temporal and spatial variations of the differential phase shift between the beams, giving two distinguishable values for the two sections, which on their own show temporal variation of a similar extent. We attribute the spatial dependence again to the second pass in the amplifier, where the pump pulse is not relay-imaged onto the BBO crystal. This can only be fixed by a new design of the NOPCPA (a substantial redesign is needed, because of the relay imaging and timing constraints).

#### 4. Conclusions

In conclusion, we have demonstrated phase- and intensity-stable double-pulse parametric amplification at the millijoule level. To measure the phase stability we employed a sensitive interferometric technique, capable of detecting single shot phase differences smaller than 10 mrad. The investigated NOPCPA laser system induces a phase shift up to  $\approx \pm 200$  mrad, depending on the operating conditions with a typical stability of 20 mrad rms over 2 minutes. The change of the phase shift during a day and between different sections of the beam typically lies within a range of 100 mrad. Because this can be monitored on line, the phase relation between the pulses is always well known.

The precision of the relative phase shift determination presented here is high enough for obtaining MHz-scale accuracy in the XUV (e.g. at the He 1s-4p transition at 52 nm or the 15<sup>th</sup> harmonic of the 780 nm). Nonlinear phase shifts in optics and the harmonic upconversion itself are of concern for such an experiment. However the observed high relative intensity stability of the two output pulses gives good prospects for high resolution Ramsey spectroscopy in the XUV.

#### Acknowledgments

We gratefully acknowledge financial support by the Netherlands Organisation for Scientific Research (NWO), the EU Integrated Initiative FP6 program Laserlab-Europe, the ATLAS EU Early Stage Training Network and by the Foundation for Fundamental Research on Matter (FOM).